Available online at www.sciencedirect.com
SCIENCE DIRECT
Catalysis Today 110 (2005) 121–131
CATALYSIS TODAY
www.elsevier.com/locate/cattod

Water-gas shift reaction in micro-channels—Results from catalyst screening and optimisation

Gunther Kolb *, Helmut Pennemann, Ralf Zapf

Institut für Mikrotechnik Mainz GmbH, Carl-Zeiss-Str. 18-20, 55129 Mainz, Germany

Available online 19 October 2005

Abstract

Wash-coated alumina catalysts introduced into micro-channels were applied for the water-gas shift reaction. The application standing behind this work was catalytic CO clean-up of reformate with the aim of hydrogen generation for mobile fuel cell systems. Bimetallic $Pt/CeO_2/Al_2O_3$, $Pt/Rh/CeO_2/Al_2O_3$, $Pt/Pd/CeO_2/Al_2O_3$ and $Pt/Ru/Al_2O_3$ catalysts were tested in a standard screening protocol under the conditions of high-temperature shift (9.1% CO, 290, 315 and 340 °C reaction temperature) and low-temperature shift (2.6% CO, 290, 315 and 340 °C reaction temperature) at a WHSV of 100 N $dm^3/(h\ g_{cat})$. Methane, was formed as the only by-product. $Pt/CeO_2/Al_2O_3$ was identified as the best candidate concerning selectivity and activity. The optimum platinum content was found to range between 3 and 5 wt.%, whereas the optimum ceria content ranged between 12 and 24 wt.%. The calcination temperature and platinum metal salt solution applied during catalyst preparation had a drastic effect on the activity of the $Pt/CeO_2/Al_2O_3$ catalyst.

Keywords: Water-gas shift; Noble metals; Micro-channels; Fuel processing

1. Introduction

Future energy generation for stationary, distributed and mobile applications will be based to a significant extend upon fuel cell technology. In short to medium term, processing of fossil fuels will play a significant role in hydrogen generation for fuel cells [1], because distribution grids already exist to supply the consumer with fossil fuels, which will support the introduction of fuel cell technology onto the market place.

In the majority of current applications, proton exchange membrane (PEM) fuel cell technology is employed. An exception is the large scale stationary power generation, where molten carbonate and solid oxide fuel cells play the major role. PEM fuel cells are, regardless of their operating temperature, sensitive to carbon monoxide. Thus a fuel processor is composed of the reformer itself and gas purification devices which may work catalytically or by membrane separation processes. Catalytic CO clean-up of all kind of fuels except for methanol requires water-gas shift reactors, whatever the CO tolerance of current PEM fuel cells may be. For conventional low-temperature PEM fuel cells, the reformate needs to be purified further by either preferential oxidation (PrOx) or methanation, the latter being a recent development [2–4].

A crucial aspect of current water-gas shift reactors is their size. They are in most cases the biggest devices of a fuel processor.

Especially for distributed, mobile and portable applications, micro-technology offers unique possibilities to run the individual stages of a fuel processor at low residence times in highly compact devices [5]. The improved heat and mass transfer of micro-structured reactors applied to heterogeneously catalysed gas phase reactions is well-known from many scientific and industrial applications nowadays [6]. However, the novel reaction conditions such as the very low residence times in micro-structured reactors create the need for adopting or even improving conventional catalyst technology according to the requirements of this new application. Conventional catalysts have been developed for processing conditions in packed beds, where generally heat and mass transport limitations dominate the reactor performance.

On top of the improved heat and mass transfer, micro-structured reactors allow for a better temperature control of the reaction, which was proven by numerical simulations to be crucial for achieving satisfactory performance [7].

* Corresponding author. Tel.: +49 6131 990 341; fax: +49 6131 990 305.
E-mail address: kolb@imm-mainz.de (G. Kolb).

0920-5861/$ – see front matter © 2005 Elsevier B.V. All rights reserved.
doi:10.1016/j.cattod.2005.09.012

This paper gives an overview of our work in the field of screening and optimisation of wash-coated catalysts in micro-channels applied for the water-gas shift reaction. However, advanced numerical simulation [8] and testing of integrated heat-exchanger/reactors for water-gas shift [9] is on its way in parallel at our laboratories.

2. Reaction system

The water-gas shift reaction:

$$CO + H_2O \rightarrow CO_2 + H_2, \quad \Delta H_{298} = -41\,\mathrm{kJ/mol} \tag{1}$$

is limited by its thermodynamic equilibrium, which may be calculated according to the formula provided below [10]:

$$K_{eq} = \exp\left(\frac{4577.8}{T} - 4.33\right) \tag{2}$$

Because subsequent CO-clean-up stages follow the shift reactor downstream as mentioned above, the CO content of water-gas shift reactor off-gas should not exceed 1 vol.%. Lower values are preferred of course but increase the size of the reactor owing to the lower reaction temperatures required from the thermodynamic equilibrium.

To limit the reactor size, water-gas shift is usually performed in two stages with intermediate cooling preferably by water injection [11]. In the first stage, the so-called high-temperature water-gas shift (HTS), most of the carbon monoxide is converted, which is performed industrially at temperatures between 350 and 450 °C. Fe_2O_3/Cr_2O_3 catalysts are applied industrially for HTS which are robust but suffer from low activity. This is less crucial for the industrial process rather than for a compact fuel processor application [12]. The second stage (low-temperature water-gas shift, LTS) is performed between 200 and 300 °C depending on the application and the CO concentration required for the product. The reaction is performed industrially over CuO/ZnO catalysts based upon alumina carrier. These catalysts are known to be sensitive to poisoning [13] and short-term temperature peaks. On top of that they are pyrophoric and thus sensitive to air exposure, which is unfavourable for fuel processor operation, especially during start-up procedures.

The application of integrated micro-structured reactors/heat-exchangers allows for adjusting a temperature profile in a single water-gas shift reactor, which then covers the whole range from HTS to LTS. This concept drives the water-gas shift reaction in a favourable direction and has significant potential for further size reductions [14].

Two reaction mechanisms are still under discussion currently for water-gas shift. One of them is the ‘‘adsorptive mechanism’’ [7]:

$$CO + H_2O \rightarrow CO_{ads} + H_2O_{ads} \rightarrow \langle int \rangle \rightarrow CO_{2,ads} + H_{2,ads} \rightarrow CO_2 + H_2 \tag{3}$$

for which the formation of surface intermediates $\langle int \rangle$ is assumed.

The other mechanism under discussion is the two-step ‘‘regenerative mechanism’’ [15–17]. This mechanism requires a redox species on the catalyst. Ceria is one of the redox species frequently applied and was therefore incorporated into the formulas below:

$$CO + s \rightarrow CO_{ads} \tag{4}$$

$$H_2O + Ce_2O_3 \rightarrow H_2 + 2CeO_2 \tag{5}$$

$$CO_{ads} + 2CeO_2 \rightarrow CO_2 + Ce_2O_3 + s \tag{6}$$

s standing for an active catalyst site. However, the formation of bidentate formate and its decomposition to hydrogen and unidentate carbonate on the catalyst surface is frequently assumed [18,19].

Another reaction taking place in parallel under the conditions of water-gas shift is the methanation reaction, which consumes valuable hydrogen:

$$CO + 3H_2 \rightarrow CH_4 + H_2O, \quad \Delta H_{298} = -283.6\,\mathrm{kJ/mol} \tag{7}$$

Finally the CO decomposition to coke or other carbonaceous species leads to catalyst deactivation, which will be discussed below.

Platinum group metals (PGM) attracted growing attention as alternative to the industrially established water-gas shift catalysts within the scope of three-way catalyst (TWC) development first. These catalysts are frequently based upon ceria carrier [20,17]. Neither ceria nor the PGM metals alone (e.g. deposited on silica or alumina) show significant activity in water-gas shift [17]. Pt/CeO_2 catalysts were found to be 15 times more active than Pt/Al_2O_3 catalysts [21]. The introduction of the noble metals onto the ceria surface creates surface defects, which promote the decomposition of the surface intermediates [18]. This leads to a similar reaction mechanism as found for ZnO [18]. Assuming the redox mechanism mentioned above, the noble metal particle size determines the metal–ceria interface, which is crucial for catalyst performance. It was even assumed that non-metallic platinum species in association with the surface ceria are responsible for the activity, at least when nano-particles are introduced onto the catalyst carrier [22].

On Pt/CeO_2 catalysts, deactivation was observed which was attributed to the formation of carbon species mostly on the ceria and partial losses of the re-oxidising potential [12,23]. The same authors observed an increase of the ceria crystallite size when the catalyst was exposed to reformate, which decreased the BET surface area. Others attribute the deactivation of Pt/CeO_2 catalysts in simulated reformate to the reduction of the ceria by large amounts of hydrogen [24]. This was rejected in a subsequent paper of another group [25], because high temperature reduction in hydrogen was found to have no effect on catalyst activity. It was rather attributed to a decrease of the active species dispersion, which was observed when the sample was exposed to pure CO at 400 °C. The ceria crystallite size remained constant during this treatment.

However, Pt/CeO_2 based catalysts containing other proprietary ingredients were developed, which show stable operation and no methanation activity [12]. Thus ceria

containing PGM catalysts, namely platinum, rhodium and palladium were regarded as promising candidates for water-gas shift and the investigations reported in this paper where focussed on such catalysts.

Few papers exist on catalyst evaluation for water-gas shift in micro-channels to-date. One of them is dealing with Ru/ZrO_2 and Au/CeO_2 catalysts [26], the other with Cu/ZnO catalysts [27].

3. Catalyst preparation

The catalyst coatings presented in this paper were prepared in-house. They were exclusively based on an alumina carrier. Completely home-made catalysts were prepared by firstly wash-coating γ-alumina onto the micro-channels from a 20 wt.% alumina suspension in deionised water. The slurry contained also 5 wt.% polyvinyl alcohol (from Fluka) as a binder and 1 wt.% acetic acid. The channels were then filled with the suspension and the excess was removed manually. The slurry inside the channels was then calcined in air for 2 h at a temperature of 600 °C. Incipient wetness impregnation was then performed with aqueous solutions of H_2PtCl_6, $Pt(NH_3)_4(OH)_2$, $RhCl_3{\cdot}H_2O$ and $RuCl_3{\cdot}H_2O$ (all purchased from ABCR), $PdCl_2$ (purchased from ACROS), $Ce(NO_3)_3{\cdot}6H_2O$ (purchased from Alfa Aesar) or mixtures of those. The samples were then calcined in air a second time at 450 or 600 °C as indicated below.

In parallel, a larger amount of catalyst was prepared in crucibles and treated exactly like the micro-channel coatings. These samples were then mechanically removed from the crucible and served as samples for physical and chemical characterisation.

For some of the catalysts prepared commercial Pt powder catalyst from Degussa (5 wt.% Pt on γ-alumina, F214 VH/D; surface area 261 m^2/g) served as a basis. The samples were then impregnated subsequently with the other species as described above.

The average thickness of the wash-coats amounted to about 30 μm.

The surface area of the samples was measured through nitrogen adsorption applying the BET method, the pore diameter by the BJH method. A SORPTOMATIC 1900 (Carlo Erba Instruments) was used for the measurements.

The metal particle size of some of the samples was measured by hydrogen pulse chemisorption with argon at 40 °C. Prior to the measurements, the samples were reduced at 450 °C with 5 vol.% hydrogen in argon.

Besides the determination of the content of metal species by weight measurements, some of the samples were analysed chemically. The chemical analysis was performed by ICP-OES.

4. Experimental

A conventional lab-scale test rig was applied for water-gas shift. The feed mixture was supplied by conventional thermal mass flow meters (BRONKHORST HI-TEC) for dosage of the gaseous components (hydrogen, carbon dioxide and carbon monoxide) and a laboratory scale evaporator (BRONKHORST CEM) for dosing and evaporating the water. Water tanks pressurised with nitrogen supplied the evaporator with liquid water. Heated lines lead from the evaporator to the reactor, to the reactor bypass-line and from there to the on-line ThermoFinnigan Trace gas chromatograph. The separation of the components was achieved by a number of columns such as a pre-column Porapak N (delays any organic molecules such as methane and water and allows the other species to enter first), a Hayesep Q (for water and carbon dioxide separation), a Molecular Sieve 5A (for separation of carbon monoxide) and a combined Hayesep and Molsieve (for hydrogen separation). Both thermal conductivity detectors employed had a temperature of 150 °C while the nitrogen carrier gas flow and the two-helium gas flows were set to a pressure at the gas chromatograph inlet of 100, 150 and 100 kPa, respectively. The gas chromatograph was programmed as follows: 8 min at 75 °C, ramp 40 °C/min to 120 °C and held for 7 min at this temperature. Thus the analytical procedure allowed for analysis of all species present in the reaction mixture including the water.

The test reactors applied have a sandwich design with two micro-structured platelets being attached face to face. The platelets carry 14 channels each, which are 25 mm long, 500 μm wide and 250 μm deep. The channels together with the inlet and outlet region were prepared by wet chemical etching. Each couple of platelets was coated with the individual carrier/catalyst system and subsequently sealed by laser welding. Inlet and outlet tubes were attached to the reactors by laser welding,

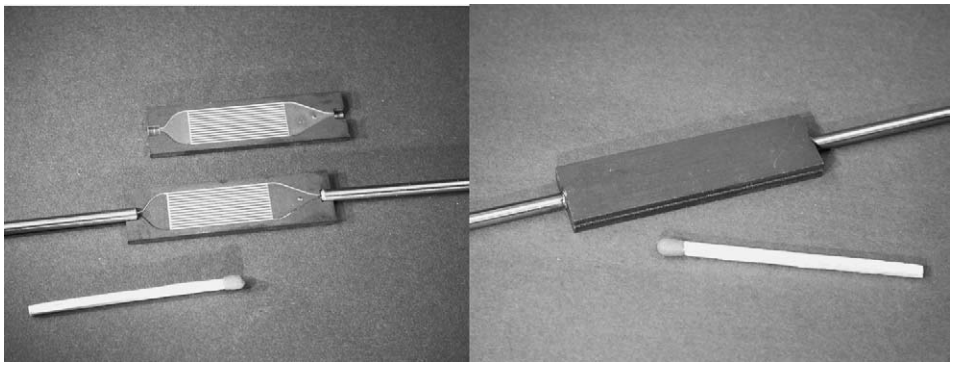

Fig. 1. Reactor applied for water-gas shift; left: coated platelets with tubing; right: platelets attached face-to-face and sealed by laser-welding.

too. Fig. 1 shows the components of the reactor before and after welding. The welding procedure did not affect the catalyst performance as described elsewhere [28].

The heating of the reactors was performed by a heating cartridge of 250 W power introduced into the borehole of a metal block. A spacer in the block covered with a plate took up the individual reactor tested. The temperature of the reactor was measured by a thermocouple positioned in another borehole between the heating cartridge and the reactor. Two further thermocouples were applied for measuring the inlet and outlet temperature of the gases. Due to the big heat capacity of the heating block and the intensive contact between the gas and the micro-channel walls, only negligible temperature differences of less than 2 °C could be measured between the gas outlet temperature and the reactor temperature. Additionally, the heating block was insulated and therefore isothermal operation of the reactor could be assumed. On top of that, an estimation of heat transfer versus heat uptake of the feed was performed elsewhere for propane steam reforming revealing isothermal operation [28]. Because the flow rates applied for the experiments performed in the scope of this paper were lower than those applied for propane steam reforming formerly and the reaction temperature was lower as well (max. 390 °C versus 750 °C), isothermal operation may well be assumed.

Mass transfer limitations were excluded, for the channel size applied here, from numerical simulations, which will be published elsewhere [8].

A pressure drop of less than 10 mbar could be measured over the reactor under all operating conditions and therefore the pressure of the experiments is regarded as ambient pressure. The pressure drop over the micro-channels was calculated to a value below 1 mbar.

Pure carbon monoxide, carbon dioxide, hydrogen and water were used as feed for the experiments.

In most experiments the water-gas shift reaction was the only reaction observed and thus only the conversion is provided below.

However, few of the catalyst samples tested showed activity towards the methanation reaction. The selectivity S_i of the carbon containing species formed was determined using the yield Y_i of each species (carbon dioxide and methane):

$$S_i = \frac{Y_i}{X_{C_3H_8}} \quad (8)$$

Other carbon containing species than carbon monoxide, carbon dioxide and methane were not measured during the experiments.

The WHSV provided below refers to the entire catalyst mass, including the alumina carrier.

5. Results

Two sets of catalyst samples were prepared in the scope of the work presented here. For the first set of samples commercial platinum catalyst served as a basis (see Section 3). The composition and the characterisation data of these catalysts are summarised in Table 1.

Table 1
Physical and chemical properties of the catalyst prepared on the basis of commercial platinum catalyst

	Sample No.			
	1	2	3	4
Metal dispersion (%)	27.3	n.d.	52.5	10.65
Surface area (m^2/g)	185	140	185	200
Mean pore diameter (nm)	4.5	n.d.	4.9	n.d.
Noble metal content (wt.%) (values from weight determination)				
Pt	4	4	4	4
Pd	–	3	–	–
Rh	–	–	4	–
Ru	–	–	–	4
Noble metal content (wt.%) (values from chemical analysis)				
Pt	3	3	3	4
Pd	–	1	–	–
Rh	–	–	2	–
Ru	–	–	–	8
Additive (wt.%) (values from weight determination)				
CeO_2	17	12	17	–
Additive (wt.%) (values from chemical analysis)				
CeO_2	14	20	15	–
Alumina carrier (mg)	15	15	15	16
Calcination temperature (°C)	600	600	600	600
Pre-treatment in air (°C)	500	500	500	500

Sample 1 was a $Pt/CeO_2/Al_2O_3$ catalyst with a target platinum content of 4 wt.%. Samples 2 and 3 were mixed $Pt/Pd/CeO_2/Al_2O_3$ and $Pt/Rh/CeO_2/Al_2O_3$ catalysts, respectively. Sample 4 was a $Pt/Ru/Al_2O_3$ catalyst containing no ceria.

All samples of this set contained about 4 wt.% of platinum according to the weight determination performed during the coating and impregnation procedure. However, chemical analysis of some of the samples revealed a lower platinum content between 2.7 and 3.6 wt.%. It is not yet clear to the authors, which analysis procedure is more precise. Losses of the noble metal during the dissolving procedure might be a possible explanation for the lower values found by chemical analysis for platinum, rhodium and palladium. However, for the ceria content both higher and lower values were found by weight determination compared to chemical analysis.

All samples had a surface area between 170 and 200 m^2/g, only for sample 2 ($Pt/Pd/CeO_2/Al_2O_3$) a lower value was found. The base powder catalyst had a significantly higher surface area of 261 m^2/g and the losses are attributed to the coating procedure. The mean pore diameter of some of the samples was determined between 4.2 and 4.9 nm. All samples presented in Table 1 were calcined in air at 600 °C both after the coating and after the impregnation procedure. Before the samples were tested under the conditions of LTS and HTS respectively they were pre-treated in air at 500 °C for 30 min. This procedure was chosen to simulate the start-up procedure of a future fuel processor. Catalyst exposure to air is almost inevitable especially in small systems and catalyst reduction prior to operation is not feasible.

Table 2
Experimental conditions applied for testing of samples 1–4 and 5–10

	Gas composition (mol%)	
	HTS	LTS
H_2	50.8	57.2
CO_2	7.7	14.3
CO	9.1	2.6
H_2O	32.3	25.8

	Equilibrium conditions					
	HTS			LTS		
Reaction temperature (°C)	340	365	390	290	315	340
Eq. conversion (%)	83	78	73	66	54	40
CO_{eq} (mol%)	1.6	2	2.4	0.9	1.2	1.6

Due to the relatively high calcination temperature of this initial set of samples, the metal dispersion, which was measured for samples 1, 2 and 4, was relatively low except for the Pt/Rh/CeO_2/Al_2O_3 catalyst (No. 3). However, these values may only serve as a basis for internal comparison.

The samples described above were tested subsequently for both LTS and HTS. Simulated reformate containing hydrogen, carbon dioxide, carbon monoxide and steam (but no methane) was applied as feed. Table 2 provides an overview of the feed compositions. The experiments were performed at three reaction temperatures subsequently (290, 315 and 340 °C for LTS and 340, 365 and 390 °C for HTS). The temperature applied for LTS does exceed the commonly applied temperature range of LTS. However, the intention of this work was to find a catalyst, which has sufficient activity under the conditions of both high and low temperature shift. Thus higher temperatures are required for LTS.

The equilibrium conversion and the corresponding minimum carbon monoxide concentration achievable under the experimental conditions applied are provided in Table 2. Four analyses were performed by the on-line GC at each temperature stage, which corresponds to a time demand of 1 h. During this short-term testing, no apparent deactivation of the samples was observed unless indicated otherwise below. The flow rate set for this initial set of experiments amounted to 30 N ml/min, which corresponds to a WHSV of about 100 N dm^3/(h g_{cat}), the precise value depending on the sample weight of course.

Fig. 2 shows the conversion as measured for samples 1–4 under the conditions of LTS. The Pt/CeO_2/Al_2O_3 sample showed higher activity compared to the Pt/Pd/CeO_2/Al_2O_3 sample. This may be attributed to the lower surface area found for the latter sample (see Table 1). However, both samples showed exclusively selectivity towards carbon dioxide since no traces of methane were detected. This was not the case for the samples containing rhodium and ruthenium. Both samples produced significant amounts of methane. The conversion of carbon monoxide exceeded even the equilibrium conversion as calculated for the water-gas shift reaction under the assumption, that this reaction took place exclusively in the reaction system. Basically the same activity ranking was measured for the HTS as indicated in Fig. 3. Table 3 shows the amount of methane found in the product and the methane selectivity of the Pt/Rh/CeO_2/Al_2O_3 catalyst. For LTS the selectivity towards methane was 85% at 340 °C reaction temperature, for HTS even 90% at 390 °C reaction temperature.

Thus the following activity ranking of the samples towards methanation was found:

$$\mathrm{Pt/Rh/CeO_2/Al_2O_3} > \mathrm{Pt/Ru/Al_2O_3} \gg \mathrm{Pt/CeO_2/Al_2O_3} \approx \mathrm{Pt/Pd/CeO_2/Al_2O_3} \approx 0$$

From literature, the following activity ranking was reported for the methanation reaction [25]:

$$\mathrm{Ru} > \mathrm{Rh} \gg \mathrm{Pt/CeO_2} \gg \mathrm{Pd/CeO_2}$$

It needs to be mentioned, that methanation started at temperatures below 300 °C for Ru and Rh [25] and had its maximum at about 500 °C, whereas it initiated at 400 °C for Pt and at 500 °C for Pd [25]. For all catalysts, the addition of ceria had no effect on methanation activity [29]. Thus the reaction temperature was

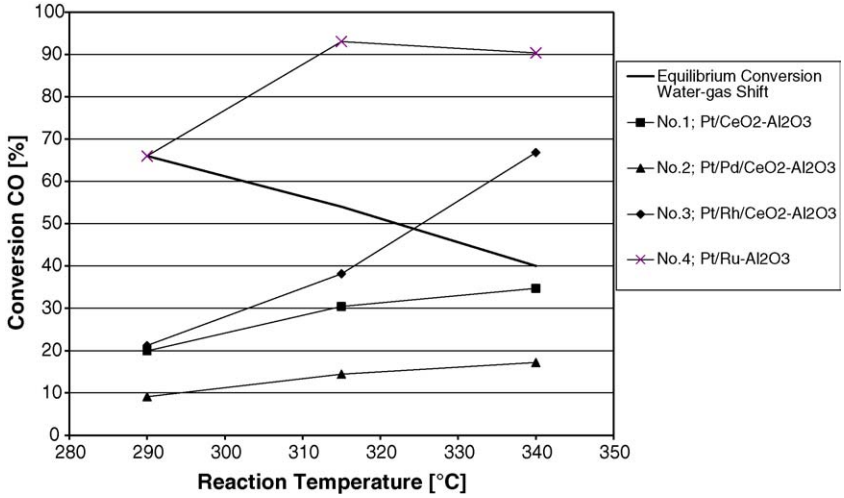

Fig. 2. CO-conversion for LTS over catalyst samples prepared from commercial Pt-catalyst; feed composition: see Table 2; total feed flow rate: 30 N cm^3/min; corresponding WHSV: 100 N dm^3/(h g_{cat}).

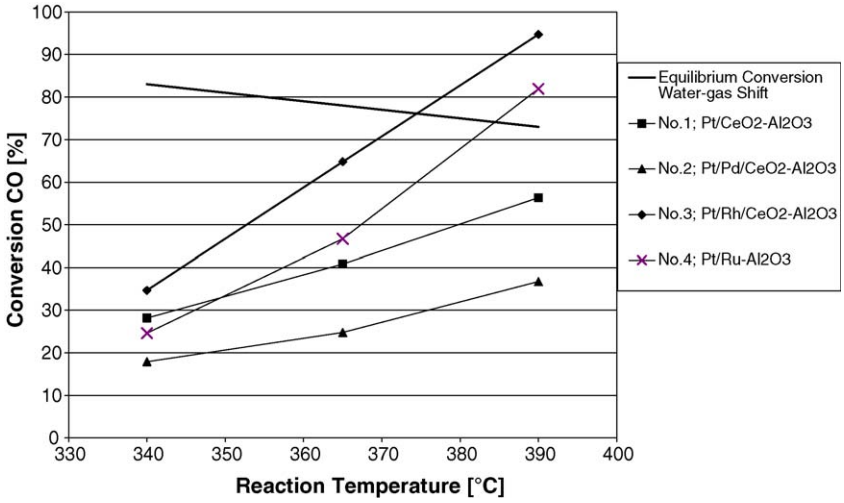

Fig. 3. CO-conversion for HTS over catalyst samples prepared from commercial Pt-catalyst (see also Table 1); feed composition: see Table 2; total feed flow rate: 30 N cm^3/min; corresponding WHSV: 100 N dm^3/(h g_{cat}).

Table 3
Conversion, selectivity towards methane and molar fraction of methane found for LTS and HTS at sample 3 (see Table 1 under the experimental conditions provided in Table 2; WHSV: 100 N dm^3/(h g_{cat})

Sample No. 3; $Pt/Rh/CeO_2$ catalyst reaction temperature (°C)	Conversion (%)	Selectivity to methane (%)	Methane molar fraction (%)
LTS			
290	21	25	0.2
315	38	60	0.6
340	67	90	1.6
HTS			
340	35	48	1.6
365	65	57	3.6
390	95	85	8.3

likely just too low for the $Pt/CeO_2/Al_2O_3$ (No. 1) and $Pt/Pd/CeO/Al_2O_3$ (No. 2) samples discussed here to show apparent methanation activity. More active, second generation $Pt/CeO_2/Al_2O_3$ catalysts, which will be discussed below, showed some activity towards methanation at temperatures close to 400 °C.

However, in the current paper bimetallic samples of $Pt/Rh/CeO_2/Al_2O_3$ (No. 3) and $Pt/Ru/Al_2O_3$ (No. 4) catalysts were under investigation. This may well be the origin of the reverse ranking for Rh and Ru compared to the literature.

The $Pt/Ru/Al_2O_3$ sample (No. 4) showed significant deactivation even during the short term test duration of 1 h, which was applied for each reaction temperature here. This deactivation is assumed to originate from coke formation. Therefore, in case of sample 4, only the initial conversion as measured for each reaction temperature is provided both in Figs. 2 and 3. The course of deactivation for LTS is shown in Fig. 4. Obviously the rate of deactivation decreases with increasing reaction temperature and gets moderate at 340 °C. At this reaction temperature, about 90% of the carbon monoxide in the feed was converted, leaving some 0.2 vol.% left in the product. However, the amount of methane formed exceeded the carbon monoxide consumption by more than

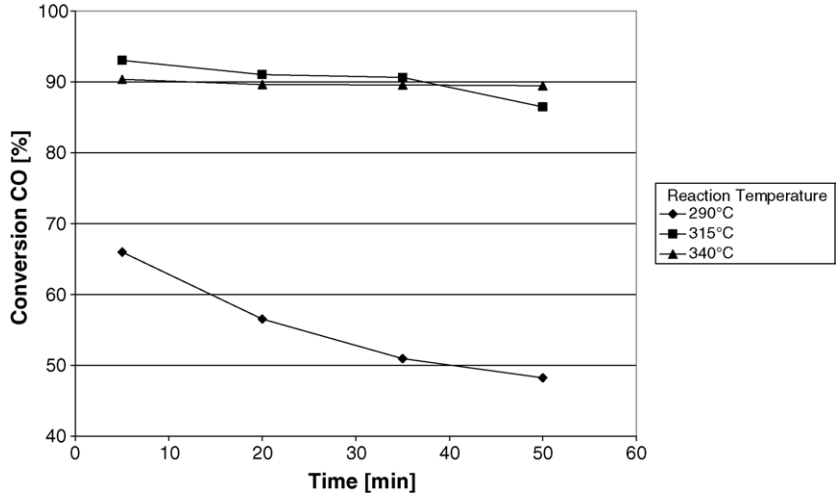

Fig. 4. CO-conversion for LTS over the $Pt/Ru/Al_2O_3$ sample 4 (see also Table 1); feed composition: see Table 2; total feed flow rate: 30 N cm^3/min; corresponding WHSV: 100 N dm^3/(h g_{cat}).

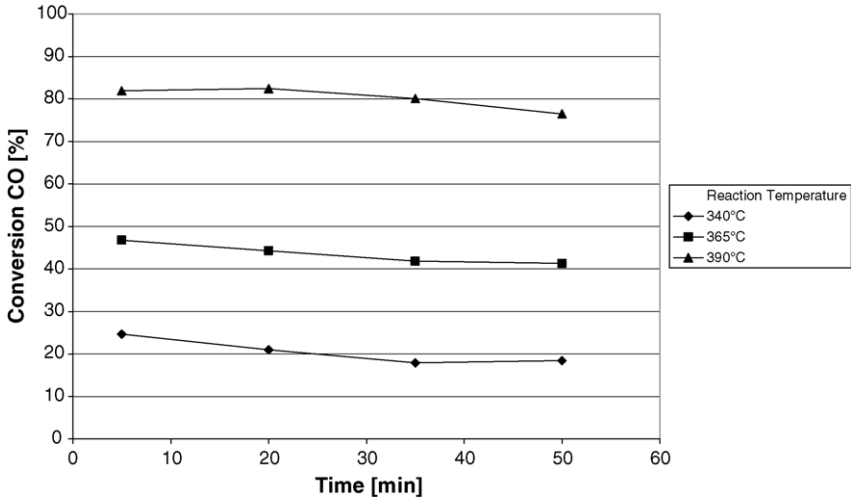

Fig. 5. CO-conversion for HTS over the $Pt/Ru/Al_2O_3$ sample 4 (see also Table 1); feed composition: see Table 2; total feed flow rate: 30 N cm^3/min; corresponding WHSV: 100 N dm^3/(h g_{cat}).

80%. Thus more methane was detected than carbon monoxide was consumed. The excess methane originated from significant carbon dioxide methanation taking place under these conditions. It could be assumed as well, that the carbon dioxide is converted to carbon monoxide via reverse water-gas shift first, which then forms methane via methanation. When switching the experimental conditions from LTS to HTS (higher content of carbon monoxide) the deactivation started again (see Fig. 5). This has to be attributed to the carbon monoxide concentration, because the same reaction temperature of 340 °C was set at the end of the LTS test and at the beginning of the HTS tests. The sample was pre-treated for 30 min at 500 °C in air prior to switching from LTS to HTS, which might have caused some re-activation of active sites by coke combustion. However, under the conditions of HTS the further increase of reaction temperature up to 390 °C did not prevent further significant deactivation of the catalyst.

Because the $Pt/Rh/CeO_2/Al_2O_3$ (No. 3) and the $Pt/Ru/Al_2O_3$ (No. 4) catalyst were highly selective towards the methanation reaction, Rh and Ru are regarded as good candidates for CO removal by methanation, which will require further optimisation of course. The combination of water-gas shift activity and methanation activity, which was found for the bimetallic catalysts under investigation here, makes their application little favourable neither for water-gas shift nor for methanation. However, they were not subject of further investigations in the scope of water-gas shift catalyst development, which is discussed in the present paper.

Wheeler determined the following activity ranking over alumina foam monoliths and a feed mixture of 11 vol.% CO,

Table 4
Physical and chemical properties of $Pt/CeO_2/Al_2O_3$ catalysts tested

	Sample no.									
	5	6	7	8	9	10	11	12	13	15
Particle size (nm)	n.d.	1.2	1.7	2.0	1.6	1.8	n.d.	n.d.	n.d.	n.d.
Metal dispersion (%)	n.d.	86	59	51	57	55	n.d.	n.d.	n.d.	n.d.
Surface area (m^2/g)	64	66	76	69	69	66	67	108	117	58
Mean pore diameter (nm)	7.0	n.d.	n.d.	n.d.	n.d.	n.d.	n.d.	n.d.	n.d.	14.0
Pt salt applied	H_2PtCl_6	H_2PtCl_6	H_2PtCl_6	H_2PtCl_6	H_2PtCl_6	H_2PtCl_6	H_2PtCl_6	–	–	$Pt(NH_3)_4(OH)_2$
Pt content (weight determination) (wt.%)	1	1	3	5	3	3	5	5	1	5
Pt Content (chemical analysis) (wt.%)	n.d.	1	3	4	1	3	n.d.	n.d.	n.d.	n.d.
CeO_2 (weight determination) (wt.%)	12	12	12	12	6	24	24	40	40	12
CeO_2 (chemical analysis) (wt.%)	n.d.	16	16	13	4	26	n.d.	n.d.	n.d.	n.d.
Alumina carrier (mg)	17	17	17	17	17	17	14	15	17	17
Base	γ-Al_2O_3	γ-Al_2O_3	γ-Al_2O_3	γ-Al_2O_3	γ-Al_2O_3	γ-Al_2O_3	γ-Al_2O_3	Commercial	Commercial	γ-Al_2O_3
Temperature calcination 1 (°C)	600	600	600	600	600	600	600	450	450	600
Temperature calcination 2 (°C)	600	450	450	450	450	450	450	450	450	450
Pre-treatment in air (°C)	500	500	500	500	500	500	450	450	450	500

23 vol.% H_2 and 46 vol.% H_2O, balance N_2, at very low space velocities below 20 ms for water-gas shift [29]:

$$Ru/CeO_2 > Pt/CeO_2 > Rh/CeO_2 > Pd/CeO_2$$

In this paper, bimetallic catalysts were prepared which showed the following ranking:

$$Pt/CeO_2/Al_2O_3 > Pt/Rh/CeO_2/Al_2O_3 > Pt/Ru/Al_2O_3 > Pt/Pd/CeO_2/Al_2O_3$$

Because the activity of the $Pt/Pd/CeO_2/Al_2O_3$ (No. 2) catalyst was lower compared to the $Pt/CeO_2/Al_2O_3$ (No. 1) catalyst and similar results were obtained by the authors for an initial set of samples not reported here [30] this type of catalyst was not investigated in depth by the authors either.

The second set of samples, which is discussed in the scope of this paper, exclusively consists of $Pt/CeO_2/Al_2O_3$ catalysts (see Table 4). Because the intention of this part of the work was to identify the optimum content of platinum and ceria and the optimum preparation route, most of these samples were prepared on the basis of γ-Al_2O_3 with subsequent impregnation of both platinum and ceria. Thus most of these samples were completely home made. Due to the lower surface area of the γ-Al_2O_3 (80 m^2/g) compared to the commercial platinum base catalyst (260 m^2/g), the surface area of these samples was consequently lower ranging between 58 and 76 m^2/g. Two calcination temperatures are provided in Table 5. The first corresponds to the calcination of the γ-Al_2O_3, the second to the calcination of the sample after impregnation.

All samples shown in Table 1, which were discussed above were prepared applying a second calcination temperature of 600 °C. However, suspicion arose, that this temperature might be too high to maintain good dispersion of the platinum. From literature, ceria-supported catalysts are known to show deterioration of their activity after high temperature calcinations despite their improved tolerance to air exposure [17]. Therefore two samples were prepared with exactly the same composition, but treated at 600 and 450 °C, respectively. As shown in Table 4, the sample treated at 450 °C after impregnation showed much higher activity. Therefore all samples prepared subsequently were calcined at 450 °C after impregnation (second calcination), which is only 60 K lower than the final reaction temperature of the test protocol (390 °C). The first calcination temperature, which was the pre-treatment of the γ-Al_2O_3, was kept at 600 °C, because no deterioration of the alumina phase was to be expected at that temperature.

Table 5
Conversion for LTS and HTS at samples 5 and 6 (see Table 4 under the experimental conditions provided in Table 2; total feed flow rate: 30 N cm^3/min; WHSV: 100 N dm^3/(h g_{cat})

Sample no.	Composition (wt.%)		Calcination temperature 2 (°C)	Conversion (%), LTS		
	Pt	CeO_2		290	315	340
5	1	12	600	7	7	12
6	1	12	450	33	49	54

Reaction temperatures are 290, 315 and 340 °C.

The next set of catalysts was prepared with different amounts of platinum and ceria. Samples 6, 7 and 8 contained 1, 3 and 5 wt.% platinum respectively along with 12 wt.% ceria. Samples 9, 6 and 10 contained 6, 12 and 24 wt.% ceria respectively along with 3 wt.% platinum (see Table 4). The metal dispersion of these samples was measured and was ranging between 51% and 86% (see Table 4), which is higher compared to the values determined for the first set of samples (see Table 1). Both metal dispersion and the corresponding metal particle size provided for the samples 6–10 was in line with their platinum content, higher platinum content revealed lower metal dispersion. Comparing the amount of platinum measured for sample 9 by weight analysis (3 wt.%) to the value from chemical analysis revealed a much lower value of 1 wt.% for the latter. However, the metal dispersion was determined to 57%, which is very similar to the values measured for the other

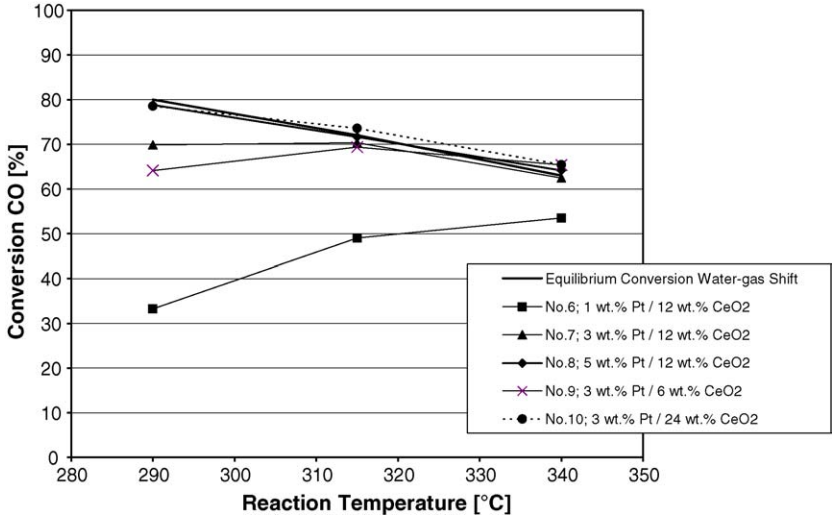

Fig. 6. CO-conversion for LTS over home-made $Pt/CeO_2/Al_2O_3$ catalyst samples; feed composition: see Table 2; total feed flow rate: 30 N cm^3/min; corresponding WHSV: 100 N dm^3/(h g_{cat}).

Table 6
Experimental conditions applied for testing of samples 7 and 9–15

	Gas composition (mol%)	
	HTS	LTS
H_2	46.8	51.8
CO_2	8.8	13.2
CO	8	3.4
H_2O	37.1	30.7

	Equilibrium conditions					
	HTS			LTS		
Reaction temperature (°C)	340	365	390	290	315	340
Eq. conversion (%)	85	81	76	80	72	63
CO_{eq} (mol%)	1.2	1.5	1.9	0.7	1	1.3

samples containing 3 wt.% platinum (Nos. 7 and 10). Thus the precision of the chemical analysis (which was perfomed externally) might be lower compared to the weight determination.

Samples 6–10 were tested according to the protocol provided in Table 2 both for LTS and HTS (see Fig. 6 for results from LTS testing). The activity of the catalysts increases both with increasing noble metal and ceria content. However, the by far lowest activity was observed for the sample containing 1 wt.% Pt, the ceria content having less significant impact on catalyst activity.

This is in line with literature, where the following ranking was observed for $Pt/CeO_2/Al_2O_3$ catalysts [29]:

$$5\%Pt/5\%CeO_2 > 1\%Pt/5\%CeO_2 > 0.2\%Pt/2\%CeO_2$$

Both sample 8 (5 wt.% Pt, 12 wt.% CeO_2) and 10 (3 wt.% Pt, 24 wt.% CeO_2) showed highest activity which was for all reaction temperatures close to the thermodynamic equilibrium under the experimental conditions applied. Under the conditions of HTS (not shown here), the distinction of the catalysts was even more difficult, because almost all samples generated thermodynamic equilibrium at all reaction temperatures under investigation.

Therefore the residence time of all experiments discussed below was decreased by about 50%. However, it was not possible experimentally, to achieve exactly the same feed composition as before for this new and higher flow-rate. The new experimental conditions are provided in Table 6.

Fig. 7 shows the results from LTS testing of the samples containing at least 3 wt.% Pt and at least 12 wt.% CeO_2. A proprietary, home-made sample was included into the data set, which outperformed the other samples significantly. The increasing activity with increasing Pt and CeO_2 content is in line with the results generated for the higher residence time. The conversion found for the sample containing 3 wt.% Pt and 24 wt.% CeO_2 (No. 10) at 340 °C is regarded as a mismeasurement. However, it is hard to distinguish the activity of the catalyst containing 5 wt.% Pt and 12 wt.% CeO_2 (No. 8) from the sample containing 5 wt.% Pt and 24 wt.% CeO_2 (No. 11).

The same activity ranking was found for HTS as shown in Fig. 8. The activity of the sample containing 5 wt.% Pt and 24 wt.% CeO_2 (No. 11) is lower or similar to the samples containing less Pt or CeO_2, which indicates, that a further increase of noble metal or CeO_2 does not help to improve the catalyst activity as long as enough CeO_2 (above 12 wt.%) is present at least under the conditions of HTS.

To further clarify the limitations of increasing the catalyst activity by increasing the ceria content, another sample (No. 12) was prepared containing 5 wt.% Pt and 40 wt.% ceria. The sample was, contrary to the other samples discussed here, prepared from commercial Pt catalyst and showed therefore a higher surface area, which should help to improve the dispersion of the active species. The temperature treatment (first and second calcination temperature) was limited to 450 °C to avoid a deterioration of the Pt dispersion. Despite this, the activity of the sample was much lower compared to the sample containing less ceria (see Table 7). However, sample No. 12 was

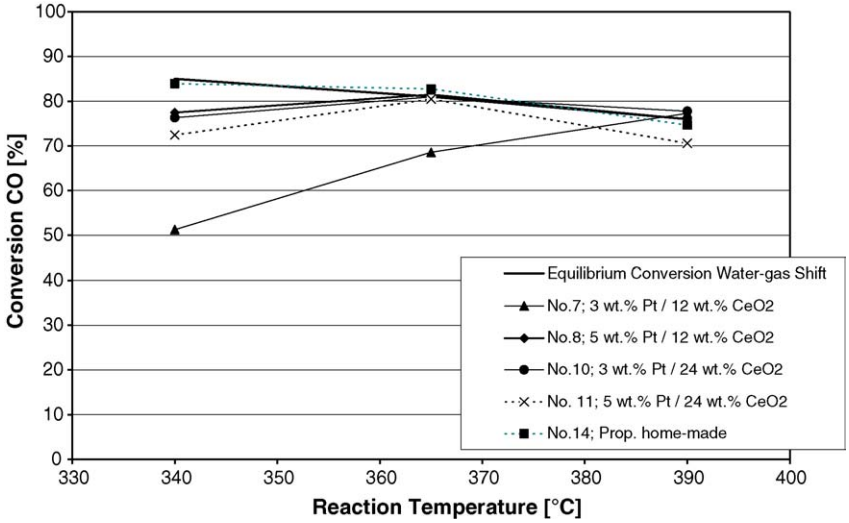

Fig. 8. CO-conversion for HTS over home-made $Pt/CeO_2/Al_2O_3$ catalyst samples; feed composition: see Table 6; total feed flow rate: 60 N cm^3/min; corresponding WHSV: 200 N dm^3/(h g_{cat}).

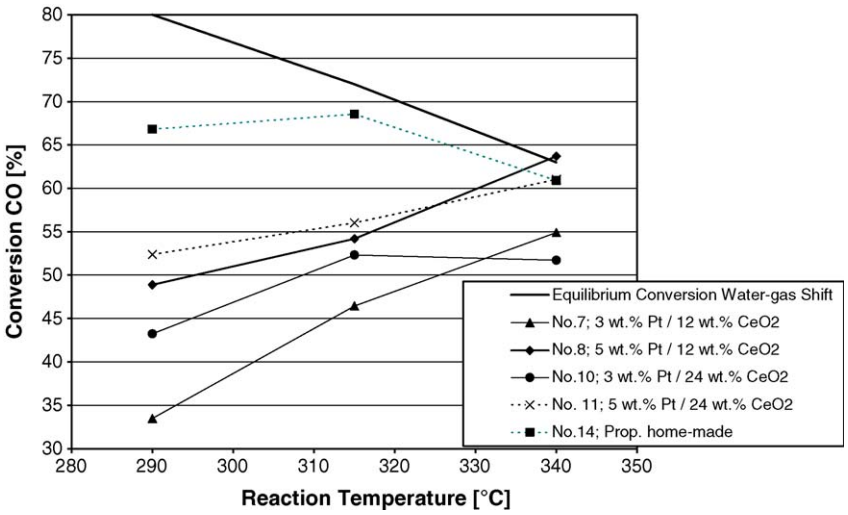

Fig. 7. CO-conversion for LTS over home-made $Pt/CeO_2/Al_2O_3$ catalyst samples; feed composition: see Table 6; total feed flow rate: 60 N cm^3/min; corresponding WHSV: 200 N dm^3/(h g_{cat}).

Table 7
CO-conversion for LTS and HTS over home-made $Pt/CeO_2/Al_2O_3$ catalyst samples; feed composition: see Table 6; total feed flow rate: 60 N cm^3/min; corresponding WHSV: 200 N dm^3/(h g_{cat})

Sample no.	Composition (wt.%)		Base type	Conversion (%)					
	Pt	CeO_2		LTS			HTS		
				290	315	340	340	365	390
8	5	12	Home-made	49	54	64	77	81	76
11	5	24	Home-made	52	56	61	72	80	71
12	5	40	Commercial	21	28	41	44	60	71

Reaction temperatures are 290, 315 and 340 °C for LTS and 340, 365 and 390 °C for HTS.

Table 9
CO-conversion for LTS and HTS over home-made $Pt/CeO_2/Al_2O_3$ catalyst samples prepared applying H_2PtCl_6 and $Pt(NH_3)_4(OH)_2$; feed composition: see Table 6; total feed flow rate: 60 N cm^3/min; corresponding WHSV: 200 N dm^3/(h g_{cat})

Sample no.	Composition			Conversion (%)					
	Pt (wt.%)	Metal salt	CeO_2 (wt.%)	LTS			HTS		
				290	315	340	340	365	390
8	5	H_2PtCl_6	12	49	54	64	77	81	76
15	5	$Pt(NH_3)_4(OH)_2$	12	22	33	52	43	63	74

Reaction temperatures are 290, 315 and 340 °C for LTS and 340, 365 and 390 °C for HTS.

prepared by impregnation of already dispersed platinum catalyst. The platinum surface might have been covered with ceria and this might have lead to a deterioration of the activity.

However, the optimum content of ceria is assumed to range between 12 and 24 wt.% for the samples prepared by co-impregnation of platinum and ceria at least for the conditions of HTS at reaction temperatures exceeding 325 °C.

Another undesired feature of samples containing 24 wt.% ceria and more is their tendency towards a certain methanation activity under the conditions of HTS at reaction temperatures exceeding 365 °C. In literature, methanation was observed as well over $Pt/CeO_2/Al_2O_3$ catalysts at temperatures exceeding 375 °C [12]. The methane content, which was measured under the conditions of HTS for samples No. 11 and 12 and for another sample containing only 1 wt.% Pt (No. 13) is provided in Table 8.

Table 8
Methane content measured for HTS over home-made $Pt/CeO_2/Al_2O_3$ catalyst samples; feed composition: see Table 6; total feed flow rate: 60 N cm^3/min; corresponding WHSV: 200 N dm^3/(h g_{cat})

Sample no.	Composition (wt.%)		Base type	Methane in off-gas (vol.%), HTS		
	Pt	CeO_2		340	365	390
11	5	24	Home-made	0.00	0.00	0.08
12	5	40	Commercial	0.00	0.00	0.02
13	1	40	Commercial	0.00	0.04	0.07

Reaction temperatures are 340, 365 and 390 °C.

Finally, the effect of the nature of the platinum precursor on catalyst activity was investigated. A set of five samples was prepared by applying $Pt(NH_3)_4(OH)_2$, whereas all home-made samples discussed above were prepared using H_2PtCl_6. In Table 9, only one couple of samples prepared by both routes is compared, however, all 5 $Pt(NH_3)_4(OH)_2$ catalysts showed lower activity compared to their H_2PtCl_6 counterpart. Metal dispersion measurements would certainly enlighten the differences but were omitted here due to financial limitations (Table 9).

6. Conclusions

$Pt/CeO_2/Al_2O_3$ seems to be the best catalyst formulation for water-gas shift, especially in case a ‘medium temperature’ (between HTS and LTS) catalyst is required, which is foreseen

to be applied in a heat-exchanger/reactor having an internal downward temperature gradient from the inlet to the outlet. An optimum concentration range of both platinum and ceria could be identified. Generally, long term stability of this catalyst type under the conditions of HTS remains an issue currently addressed in our laboratories.

References

[1] Strategic Research Agenda of the European Hydrogen and Fuel Cell Technology Platform, https://www.hfpeurope.org/uploads/677/686/HFP-SRA004_SRA-report-draft_08DEC2004.pdf.
[2] M. Echigo, T. Tabata, J. Chem. Eng. Jpn. 37 (2004) 75.
[3] S. Takenaka, T. Shimizu, K. Otsuka, Int. J. Hydrogen Energy 29 (2004) 1065.
[4] T. Utaka, T. Takeguchi, R. Kikuchi, K. Eguchi, Appl. Catal. A: Gen. 246 (2003) 117.
[5] V. Hessel, H. Löwe, A. Müller, G. Kolb, Chemical Micro Process Engineering-Processing, Applications and Plants, Wiley, Weinheim, 2005, p. 281 ff, ISBN 13 978-3-527-30998-6.
[6] G. Kolb, V. Hessel, Chem. Eng. J. 98 (2001) 1.
[7] Y. Choi, H.G. Stenger, J. Power Source 124 (2003) 432.
[8] T. Baier, K. Drese, G. Kolb, V. Hessel, H. Löwe, Numerical simulations to assess the benefits of integrating heat-exchanging capabilities into a water-gas shift reactor, in preparation.
[9] J. Schürer, G. Kolb, D. Tiemann, V. Hessel, H. Löwe, Results from testing micro-structured water-gas shift and preferential oxidation reactors designed for a 5 kW fuel processor operated with iso-octane, in preparation.
[10] J.M. Moe, Chem. Eng. Pro. 58 (1962) 33.
[11] M.V. Twigg (Ed.), Catalyst Handbook, 2nd ed., Wolfe Press, London, 1989, , Chapter 6: 'Water-gas shift'.
[12] A.F. Ghenciu, Curr. Opin. Solid State Mater. Sci. 6 (2002) 389.
[13] M.V. Twigg, M.S. Spencer, Appl. Catal. A: Gen. 212 (2001) 161.
[14] W.E. TeGrotenhuis, D.L. King, K.P. Brooks, B.J. Holladay, R.S. Wegeng, in: Proceedings of the Sixth International Conference on Microreaction Technology, AIChE, NY, 2002), p. 18.
[15] T. Bunluesin, R.J. Gorte, G.W. Graham, Appl. Catal. B: Environ. 15 (1998) 107.
[16] Y. Li, Q. Fu, M. Flytzani-Stephanopoulos, Appl. Catal. B: Environ. 27 (2000) 179.
[17] S. Hilaire, X. Wang, T. Luo, R.J. Gorte, J. Wagner, Appl. Catal. A: Gen. 215 (2001) 271.
[18] T. Shido, Y. Iwasawa, J. Catal. 141 (1993) 71.
[19] F.H.M. Dekker, M.C. Dekker, A. Bliek, F. Kapterijn, J.A. Moulijn, Catal. Today 20 (1994) 409.
[20] L. Mendelovici, M. Steinberg, J. Catal. 96 (1985) 285.
[21] N. Koryabkina, F. Ribeiro, W. Ruettinger, Fuel cell technology: opportunities and challenges, in: Proceedings of the AIChE Spring Meeting, New Orleans, 2002), p. 92.
[22] Y. Li, Q. Fu, M. Flytzani-Stephanopoulos, Science 301 (2003) 935.
[23] A. Goguet, F. Meunier, J.P. Breen, R. Burch, M.I. Petch, A.F. Ghenciu, J. Catal. 226 (2004) 382.
[24] J.M. Zalc, V. Sokolovskii, D.G. Löffler, J. Catal. 206 (2002) 169.
[25] X. Wang, R.J. Gorte, J.P. Wagner, J. Catal. 212 (2002) 225.
[26] O. Goerke, P. Pfeifer, K. Schubert, Appl. Catal. A: Gen. 263 (2004) 11.
[27] G. Germani, A.S. Quiney, A. van Veen, Y. Schuurman, C. Mirodatos, G. Kolb, in: Proceedings of the Seventh International Conference on Microreaction Technology, Lausanne, 2003), p. 173, Book of abstracts.
[28] G. Kolb, R. Zapf, V. Hessel, H. Löwe, Appl. Catal. A: Gen. 277 (2004) 155.
[29] C. Wheeler, A. Jhalani, E.J. Klein, S. Tummala, L.D. Schmidt, J. Catal. 223 (2004) 191.
[30] G. Kolb, R. Zapf, H. Pennemann, V. Hessel, H. Löwe, Wash-coat catalysts applied for the water-gas shift reaction in micro-channels, in: Proceecings of the AIChE Spring Meeting, New Orleans, 25–29 April 2004 published on CD, Paper 2d, 2004.